

# Electrodeposition of gallium and zinc onto aluminium. Influence of the electrodeposited metals on the activation process

D.O. Flamini, S.B. Saidman<sup>\*</sup>, J.B. Bessone<sup>1</sup>

*Instituto de Ingeniería Electroquímica y Corrosión (INIEC), Departamento de Ingeniería Química, Universidad Nacional del Sur,  
Av. Alem 1253, 8000 Bahía Blanca, Argentina*

Received 10 July 2006; received in revised form 13 February 2007; accepted 2 April 2007  
Available online 11 April 2007

## Abstract

The electrodeposition of gallium and/or zinc on aluminium, aluminium–zinc alloy and vitreous carbon electrodes in chloride solutions is analysed. The electrodisolution of the formed interfaces is also described and discussed. For this purpose, potentiodynamic and potentiostatic techniques and open circuit potential measurements were employed and surface characterisation was performed by scanning electron microscopy and energy dispersive X-ray analysis. The presence of zinc, electrodeposited from the solution or as an alloying component, facilitates gallium enrichment at the interface and improves the wetting on the aluminium oxide. These conditions ensure the formation of a surface Ga–Al amalgam. As a result, the dissolution process occurs at potentials which are more active than those observed for aluminium or aluminium–zinc alloy in halide solutions.

© 2007 Elsevier B.V. All rights reserved.

*Keywords:* Electrodeposition; Aluminium; Gallium; Zinc; Activation mechanism

## 1. Introduction

Aluminium is the most commonly used sacrificial material for cathodic protection of steel in sea water. Pure aluminium supports a thin protective oxide film which makes it useless as a pure metal sacrificial anode. The addition of alloying elements such as In, Ga, Hg, Sn, Zn, shifts the pitting potential towards more negative potentials [1], causing the so-called activation of Al. These elements can exert a similar activating effect when they are present as metal ions in the electrolyte [2,3]. Ternary alloys also containing Zn are usually used for sacrificial anodes. The presence of Zn improves the efficiency and produces a positive shift in the operation potential compared with the corresponding binary alloy [4–6]. In the case of gallium, higher concentrations of the metal are required to produce activation compared with the other elements [7–9]. Gallium can be deposited onto Al surfaces by cathodic polarisation at  $-2.0$  V in chloride solution containing  $\text{Ga}^{3+}$  [7], but complete activation is

not achieved. The activating effect of Ga is considered to be related with the increased adsorption of chloride ions at more negative potentials [7,10]. It has also been proposed that the activation of Al–Ga alloys in chloride media is associated with Ga particles at the metal/oxide interface [11]. These particles cause local thinning of the passivating film and then Al from the alloy diffuses rapidly through the Ga prior to its oxidation.

In a previous paper it was reported that a very negative potential was measured when an Al–Zn alloy was introduced to an aerated chloride or acetic acid solution containing  $\text{In}^{3+}$  [12]. A similar activation was found when metallic gallium was mechanically attached to Al [13]. The effect was explained considering that an amalgam is formed, which detaches the oxide film and avoids repassivation. Depending on whether the metal (In or Ga) at the active interface is solid or liquid, two activation mechanisms of Al dissolution are operative: i) when a sufficient amount of the metal (In or Ga) at quasi-liquid state is present, an amalgam is responsible for the activation process (near  $-1.4$  V) and ii) at higher anodic potentials (near  $-1.1$  V) where the presence of solid Ga (saturated amalgam) at the interface facilitates a chloride adsorption process which depolarises the anodic reaction.

<sup>\*</sup> Corresponding author. Tel./fax: +54 291 4595182.

E-mail address: [ssaidman@criba.edu.ar](mailto:ssaidman@criba.edu.ar) (S.B. Saidman).

<sup>1</sup> Professor J.B. Bessone died on 23rd April 2006.

Table 1  
Electrode composition

Sample	Zn wt.%	Si ppm	Fe ppm	Cu ppm
Pure Al	–	5	4	3
Al–4% Zn	3.86	152	70	31

The aim of the present work is to get a better knowledge of the activation process of Al alloys. In this sense, the earlier work was extended by analysing the effects of Ga and Zn on the activation of Al. To address these issues three systems were analysed in chloride solution: Al or vitreous carbon electrodes in the presence of  $Zn^{2+}$  and  $Ga^{3+}$  and Al–Zn alloy in the presence of  $Ga^{3+}$ . The cathodic polarisation of Al in acidic solutions in the presence of  $Ga^{3+}$  and  $Zn^{2+}$  can be used as a method to generate surface conditions similar to those found in the ternary alloys. Because the study of the codeposition of  $Ga^{3+}$  and  $Zn^{2+}$  ions onto Al is complicated by the presence of the Al oxide, a better assessment of the interaction between Zn and Ga can be obtained by studying the electrodeposition of both ions onto an inert substrate, in this case vitreous carbon.

## 2. Experimental details

Disc electrodes made from aluminium, aluminium–zinc alloy and vitreous carbon rods embedded in a Teflon holder with an exposed area of  $0.07\text{ cm}^2$  were used as working electrodes. The electrode compositions are presented in Table 1. The discs were polished with 1000 grit SiC emery paper followed by  $1\text{ }\mu\text{m}$  and  $0.3\text{ }\mu\text{m}$  grit alumina suspensions and then cleaned with triply distilled water. The auxiliary electrode was a large Pt sheet. Potentials were measured against an SCE reference electrode connected through a Luggin–Haber capillary tip and so are given throughout this work.

Measurements were performed in  $0.5\text{ M NaCl}$  solutions containing  $0.01\text{ M Ga}^{3+}$  and/or  $0.01\text{ M Zn}^{2+}$  in a purified

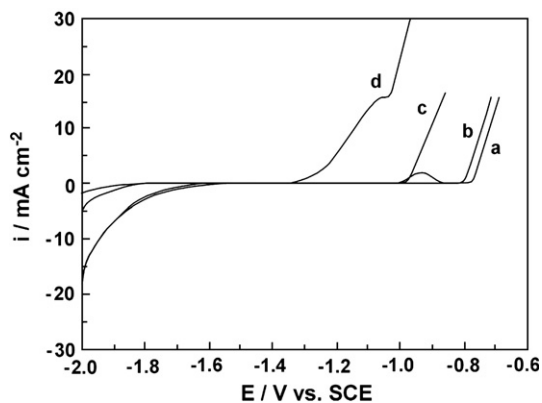


Fig. 1. Potentiodynamic polarisation of Al at  $0.005\text{ V s}^{-1}$  after cathodic polarisation at  $-2.0\text{ V}$  during 10 min in a  $0.5\text{ M NaCl}$ , pH 2.5 solution in the presence of different concentrations of  $Ga^{3+}$  and  $Zn^{2+}$ : (a) without  $Ga^{3+}$  and  $Zn^{2+}$ , (b)  $0.01\text{ M Zn}^{2+}$ , (c)  $0.01\text{ M Ga}^{3+}$  and (d)  $0.01\text{ M Zn}^{2+} + 0.01\text{ M Ga}^{3+}$ .

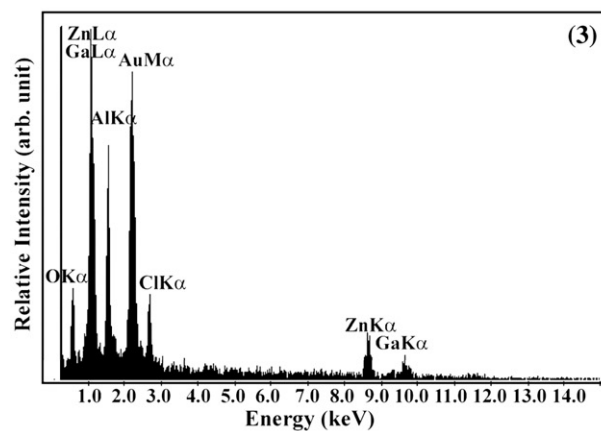
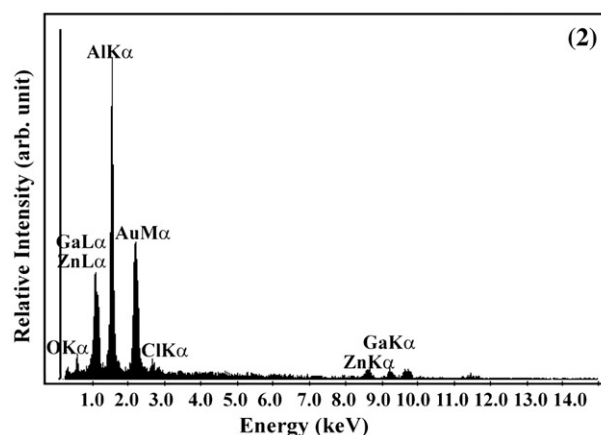
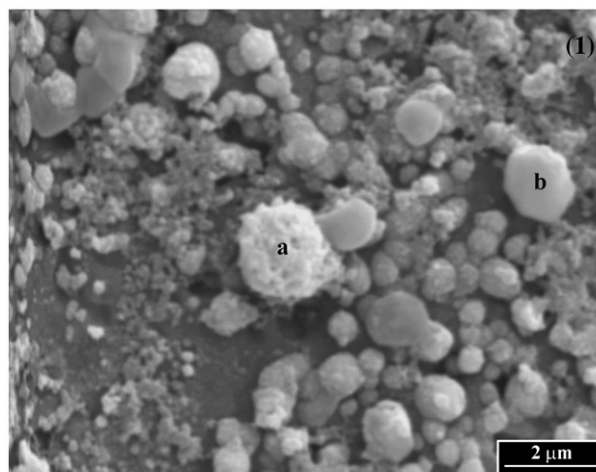


Fig. 2. (1) SEM micrograph showing the deposit obtained after cathodic polarisation of Al at  $-2.0\text{ V}$  during 10 min in a  $0.5\text{ M NaCl}$ , pH 2.5 solution containing  $Ga^{3+}$  and  $Zn^{2+}$  ions; (2) EDX spectrum of the spherical deposit shown in point a and (3) EDX spectrum of the hexagonal deposit shown in point b.

nitrogen gas saturated atmosphere at  $25\text{ }^\circ\text{C}$ . The pH was adjusted to 2.5 by addition of HCl. All chemicals were analytical grade.

Potentiodynamic, potentiostatic and open circuit-time experiments were performed with a potentiostat–galvanostat PAR Model 273A. A dual stage ISI DS 130 scanning electron microscope (SEM) (JEOL 35 CF, Japan) operated at  $15\text{ kV}$  and a quantitative energy dispersive X-ray (EDX) analyser (EDAX-DX 4, USA) were used to examine the surface characteristics of gold metalised electrodes.

### 3. Results

#### 3.1. Aluminium electrode

Fig. 1 shows the potentiodynamic anodic polarisation for an Al electrode at  $0.005 \text{ V s}^{-1}$  after cathodic polarisation at  $-2.0 \text{ V}$  in  $0.5 \text{ M Cl}^-$ , pH 2.5 solution containing  $\text{Ga}^{3+}$  and/or  $\text{Zn}^{2+}$  and the response corresponding to the blank solution. The curve obtained in the presence of  $\text{Ga}^{3+}$  presents a current increase associated with the pitting process which occurs at more negative potentials than that corresponding to bare Al. This pitting potential shift was explained considering that the presence of deposited Ga changes the chloride adsorption potential on the Ga–Al interface [7,13]. In the case of  $\text{Zn}^{2+}$  the current increase is preceded by a peak related to Zn oxidation.

When both ions were electroreduced the posterior anodic scan presented an anodic peak initiating at  $-1.35 \text{ V}$  followed by a current increase.

SEM/EDX examination of the electrode surface after cathodisation in the presence of  $\text{Zn}^{2+}$  and  $\text{Ga}^{3+}$  reveals spherical deposits with a higher content of Ga (55 wt.%) and hexagonal platelets with a higher content of Zn (65 wt.%) (Fig. 2). It looks as if the Ga electrodeposits increase over the earlier Zn nuclei.

Fig. 3 shows the open circuit potential (OCP) vs. time of an Al electrode which has been polarised at  $-2.0 \text{ V}$  in the same solutions presented in Fig. 1. A chloride pitting activation process takes place once the chloride adsorption potential on Ga is overcome near  $-1.1 \text{ V}$ . It can be observed that very negative potentials were measured for the solution containing  $\text{Zn}^{2+}$  but this activation cannot be maintained and the OCP tends to more positive values. In contrast, when both ions are present the OCP remains at very negative values for a longer time.

#### 3.2. Al–Zn alloy electrode

Fig. 4 shows the potentiodynamic anodic polarisation at  $0.005 \text{ V s}^{-1}$  for an Al–4% Zn electrode after cathodic polarisation at  $-2.0 \text{ V}$  in a  $0.5 \text{ M Cl}^-$ , pH 2.5 solution with and without  $0.01 \text{ M Ga}^{3+}$ . In the absence of  $\text{Ga}^{3+}$  the pitting

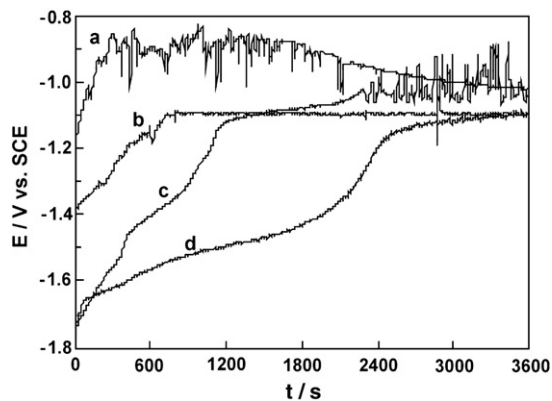


Fig. 3. Open circuit potential of Al after cathodic polarisation at  $-2.0 \text{ V}$  during 10 min in a  $0.5 \text{ M NaCl}$ , pH 2.5 solution in the presence of different concentrations of  $\text{Ga}^{3+}$  and  $\text{Zn}^{2+}$ : (a) without  $\text{Ga}^{3+}$  and  $\text{Zn}^{2+}$ , (b)  $0.01 \text{ M Ga}^{3+}$ , (c)  $0.01 \text{ M Zn}^{2+}$  and (d)  $0.01 \text{ M Zn}^{2+} + 0.01 \text{ M Ga}^{3+}$ .

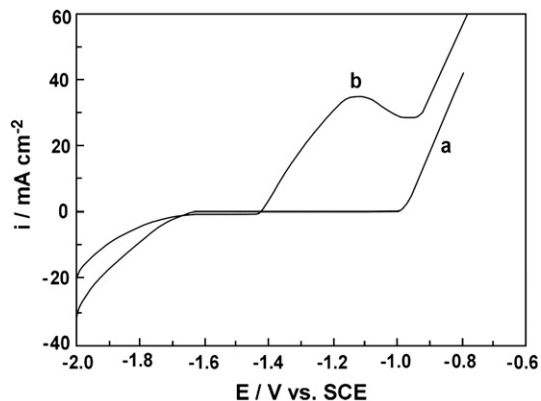


Fig. 4. Potentiodynamic polarisation of Al–4% Zn at  $0.005 \text{ V s}^{-1}$  after cathodic polarisation at  $-2.0 \text{ V}$  during 10 min in a  $0.5 \text{ M NaCl}$ , pH 2.5 solution: (a) without  $\text{Ga}^{3+}$  and (b) containing  $0.01 \text{ M Ga}^{3+}$ .

potential is observed at  $-0.98 \text{ V}$  (Fig. 4, curve a). In the presence of Ga deposited from the solution during the polarisation at  $-2.0 \text{ V}$ , a current peak beginning at  $-1.4 \text{ V}$  is obtained preceding a sharp current increase (Fig. 4, curve b). This peak is also observed when the electrode is rotated during the potential scan. The current increase at the more positive potentials is due to the

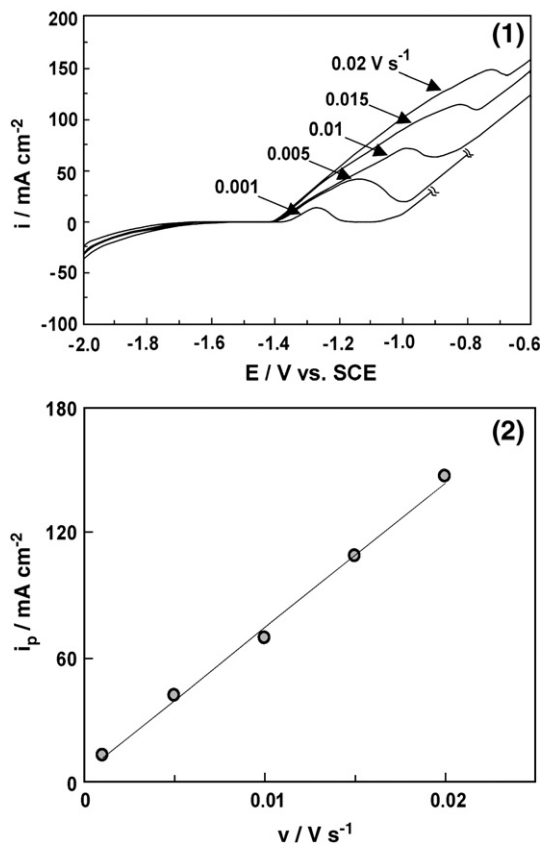


Fig. 5. (1) Potentiodynamic polarisation at different scan rates ( $v$ ) of Al–4% Zn after cathodic polarisation at  $-2.0 \text{ V}$  during 10 min in a  $0.5 \text{ M NaCl}$ , pH 2.5 solution containing  $0.01 \text{ M Ga}^{3+}$ ; (2) Plot of peak current ( $i_p$ ) against  $v$  derived from voltammetric data.

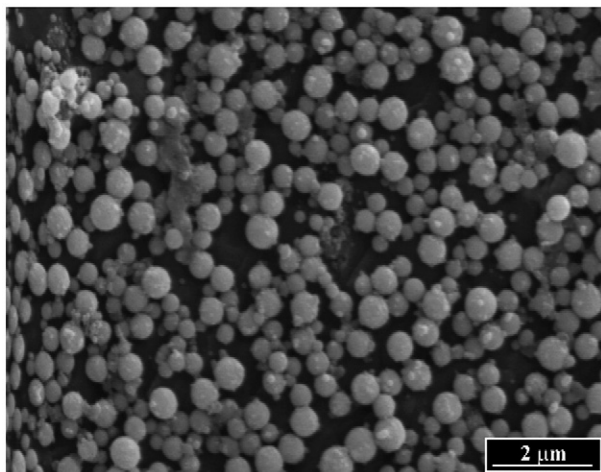


Fig. 6. SEM micrograph showing the deposit obtained after cathodic polarisation of Al-4% Zn at  $-2.0$  V during 10 min in a 0.5 M NaCl, pH 2.5 solution containing  $\text{Ga}^{3+}$  ions.

Al pitting process sustained by the chloride adsorption catalysed by Ga from  $-1.2$  V onwards [7,13]. Considering the potential region where the current peak appears, the oxidation current

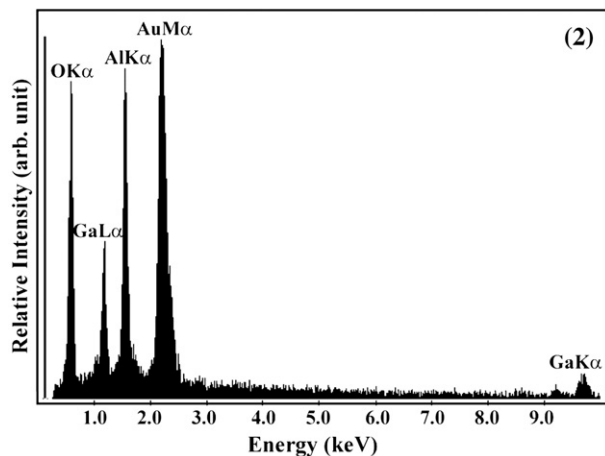
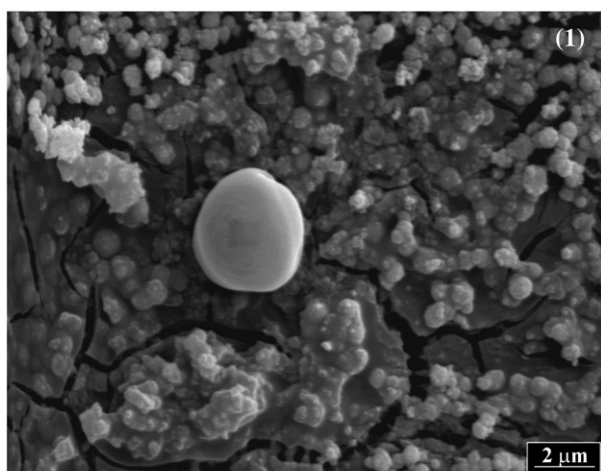


Fig. 7. (1) SEM micrograph showing the electrode surface of Al-4% Zn after the anodic peak shown in Fig. 4b was registered, and (2) EDX spectrum of the big spherical particle.

changes from milliamperes to microamperes when the systems with and without  $\text{Ga}^{3+}$  ions are compared.

A linear relationship between the peak current and sweep rate was found (Fig. 5) indicating, in principle, the participation of a surface process in the course of the anodic reaction. The electrode surface was analysed by SEM/EDX by selecting potentials before and after the current peak. The micrograph obtained after polarisation at  $-2.0$  V (Fig. 6) indicates an increase in the number of Ga nuclei and the formation of more homogeneous deposits by comparison with those obtained when Al is used as a substrate. A cracked structure was observed in some areas of the electrode surface after the anodic peak was registered (Fig. 7). Big spherical particles of Ga are seen in between the disrupted film. The EDX analysis of the particle also shows the presence of Al.

Comparing the OCP vs. time measurements obtained for an Al-Zn alloy after polarisation at  $-2.0$  V in a chloride solution with and without  $\text{Ga}^{3+}$  ions, a more negative value was measured in the presence of  $\text{Ga}^{3+}$  (Fig. 8). After a period of 350 s the potential shifted positive to the value corresponding to the bare Al-Zn alloy.

Another experiment was performed placing a gallium particle on top of a hole drilled in the Al-Zn electrode. The electrode was immersed in a 0.5 M NaCl solution of pH 2.5 and the open circuit potential vs. time was followed. This potential dropped rapidly to a very active value ( $-1.71$  V) where it remained. Finally, after a period of approximately 10 min, the whole electrode was disintegrated into numerous fragments.

### 3.3. Vitreous carbon electrode

Fig. 9.1 shows the potentiodynamic runs at  $0.02$  V  $\text{s}^{-1}$  in a 0.5 M  $\text{Cl}^-$ , pH 2.5 solution in the presence of  $0.01$  M  $\text{Ga}^{3+} + 0.01$  M  $\text{Zn}^{2+}$ , those obtained in the presence of only one cation and Fig. 9.2 that corresponding to the blank solution. It can be observed that the deposition of Ga occurs at more negative potentials than those corresponding to Zn. In the presence of both ions a reduction peak located between those peaks corresponding to individual ions is observed. When the potential sweep is reversed only the Zn oxidation peak is shown. Comparing both anodic peaks, that

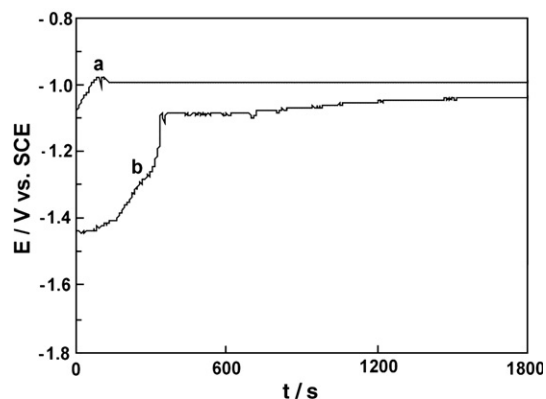


Fig. 8. Open circuit potential of Al-4% Zn after cathodic polarisation at  $-2.0$  V during 10 min in a 0.5 M NaCl, pH 2.5 solution: (a) without  $\text{Ga}^{3+}$  and (b) containing  $0.01$  M  $\text{Ga}^{3+}$ .



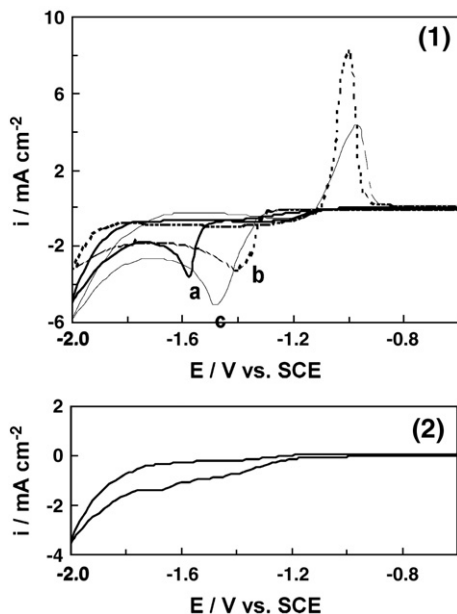


Fig. 9. (1) Potentiodynamic polarisation of vitreous carbon at  $0.02 \text{ V s}^{-1}$  in a  $0.5 \text{ M NaCl}$ ,  $\text{pH } 2.5$  solution containing: (a)  $0.01 \text{ M Ga}^{3+}$ , (b)  $0.01 \text{ M Zn}^{2+}$ , (c)  $0.01 \text{ M Ga}^{3+} + 0.01 \text{ M Zn}^{2+}$ , and (2) without  $\text{Zn}^{2+}$  and  $\text{Ga}^{3+}$ .

coming only from deposited Zn presents a symmetric, more reversible event, while that coming from both deposited metals, presents a lower charge and an abrupt current interruption.

In the presence of  $\text{Ga}^{3+}$  and  $\text{Zn}^{2+}$  the current transient at  $-1.48 \text{ V}$  clearly shows the appearance of two peaks (Fig. 10, curve a), which may be considered as the sum of Zn and Ga deposition. This fact can be deduced from the SEM/EDX analysis. Surface examination after 120 s of polarisation at  $-1.48 \text{ V}$  shows small particles (75 wt.% of Ga and 25 wt.% of Zn) and bigger particles on top (85 wt.% of Ga and 15 wt.% of Zn) (Fig. 11), indicating that the Ga content increases as the deposition time increases. The initial part of the transient is similar to that obtained in the presence of only  $\text{Zn}^{2+}$  (Fig. 10, curve b), corroborating that Zn electrodeposition prevails in the early stages of cathodisation. On the other hand, in the

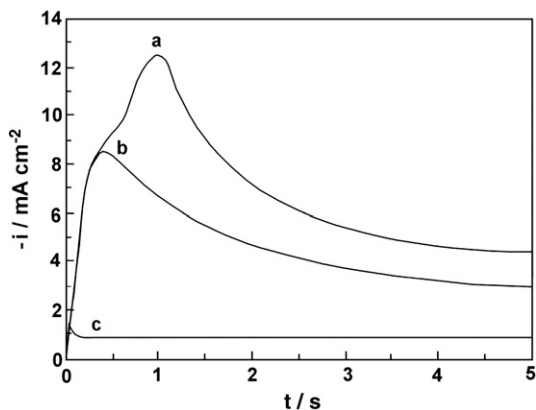


Fig. 10. Potentiostatic current transient at  $-1.48 \text{ V}$  in a  $0.5 \text{ M NaCl}$ ,  $\text{pH } 2.5$  solution containing: (a)  $0.01 \text{ M Ga}^{3+} + 0.01 \text{ M Zn}^{2+}$ , (b)  $0.01 \text{ M Zn}^{2+}$  and (c)  $0.01 \text{ M Ga}^{3+}$ .  $E_i = -0.8 \text{ V}$ .

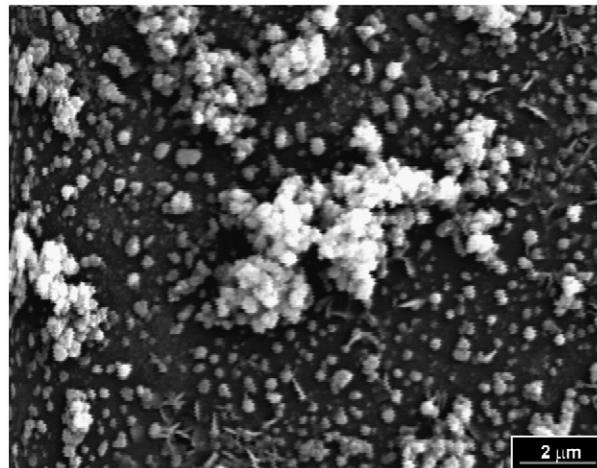


Fig. 11. SEM micrograph of the deposit obtained in a  $0.5 \text{ M NaCl}$ ,  $\text{pH } 2.5$  solution containing  $0.01 \text{ M Ga}^{3+} + 0.01 \text{ M Zn}^{2+}$  after 120 s of polarisation at  $-1.48 \text{ V}$ .

absence of  $\text{Zn}^{2+}$ , no Ga deposits have been found under the same experimental conditions (Fig. 10, curve c).

#### 4. Discussion

The experimental findings obtained in the present work can be interpreted on the basis of substrate dissolution through an amalgam-activation mechanism. It is considered that once a critical surface concentration of Ga in the liquid state and in metallic contact with Al is achieved; wetting of Al facilitates the formation of this amalgam [13]. The current peak initiating at  $-1.4 \text{ V}$  (Fig. 4, curve b) is probably related to the Al diffusion through the amalgam.

It is known that oxidation of Ga takes place in the potential zone corresponding to the anodic peak when it is polarised in very alkaline solutions [11]. A pH increase is expected to take place as a consequence of the local alkalisation produced during cathodisation [14]. A local alkalisation in the potential range corresponding to the anodic peak shown in Figs. 1 and 4 is unlikely. Therefore, this peak cannot be attributed to the oxidation of deposited gallium when the potentiodynamic run is recorded after cathodisation [15]. Anyway, an anodic peak similar to that in Fig. 4, curve b was found if after polarisation at  $-2.0 \text{ V}$  the Al–Zn electrode was rotated. Under this condition the pH at the electrode interface is similar to that in the bulk solution, that is, the possibility of local alkalisation disappears. On the other hand, the fact that a similar activating effect is also produced by In [12] constitutes evidence that the process is not associated with Ga oxidation.

Experiments using vitreous carbon as a substrate indicate that during cathodisation Zn favours Ga enrichment at the interface (Fig. 11). When some Zn nuclei are deposited  $\text{Ga}^{3+}$  can adsorb on these nuclei. The reduction of  $\text{Ga}^{3+}$  species is also probably enhanced by the presence of Zn due to a galvanic reaction if the working potential is anodic for the  $\text{Zn}/\text{Zn}^{2+}$  couple.

The anodic peak found when Al–Zn alloy is used as a substrate (Fig. 4, curve b) does not appear when Ga is deposited

on pure Al (Fig. 1, curve b). The presence of Zn (in the Al–Zn alloy or deposited during cathodisation) facilitates the deposition of Ga. Thus, the amount of Ga deposited would be higher, reaching the critical concentration needed to activate the Al oxidation through the amalgam formation. Depassivation follows and the anodic dissolution of Al is secured. On the other hand, it has been found that the addition of a small percentage of Zn to Hg renders the wetting action on Al oxide more effective [16]. Thus, the presence of Zn probably also facilitates the Ga wetting on Al oxide.

The surface structure developed after the anodic peak was registered appears as a result of an active interface. A cracked corrosion product was observed similar to that obtained when metallic Ga was mechanically attached to Al [13]. The formation of big spherical particles of Ga, probably as a result of the coalescence of smaller deposits, supports the existence of liquid Ga during the activation process. The presence of Al in the particle detected by EDX (Fig. 7) constitutes another evidence of the amalgam formation. Thus, this type of morphology is consistent with the amalgam-activation followed by a rapid passivation [13]. This passivation is related to amalgam saturation and solidification. The incorporation of Ga as an alloying element to highly pure Al causes that passivation of Al completely disappears in a chloride solution [17].

The activation by amalgam depassivation control requires a sufficient amount of the metal (Ga or In) at quasi-liquid state. During activation the temperature is maintained high enough by the  $\text{Al}^{3+}$  hydrolysis reaction. Because of the low melting point of Ga the anodic peak appears when Ga and Zn are codeposited onto Al (Fig. 1, curve d). In contrast, the activation at very negative potentials is absent when In and Zn are electrodeposited [18].

Liquid metal embrittlement of Al by liquid Ga is a well known phenomenon [19,20]. The surface of solid Al is wet by liquid Ga, which spontaneously penetrates into the grain boundaries. This process occurs when liquid Ga wets the surface of Al. The presence of Zn evidently facilitates the penetration of Ga, leading to a catastrophic attack when a Ga particle is in contact with the Al–Zn alloy.

## 5. Conclusions

The present results indicate that an accelerated deposition of Ga occurs once Zn is deposited onto Al or when an Al–Zn alloy is used as a substrate. Studies performed with vitreous carbon corroborate that zinc facilitates the deposition of Ga.

The electrodeposited Ga and Zn on Al caused the initiation of a dissolution process in chloride solutions at very negative potentials. From the results presented it is clear that this anodic process is not due to Ga oxidation. The obtained results are interpreted on the basis of an amalgam-activation mechanism. The degree of activation depends on the amount of Ga accumulated on the Al surface and its liquid or solid state. Due to the presence of Zn, the critical surface concentration of Ga needed to wet and to facilitate the formation of the Ga–Al amalgam is assured. The present results allow us to propose that the presence of zinc-rich zones in the ternary alloy favours Ga enrichment at the interface by a displacement reaction.

## Acknowledgments

The financial support of the Secretaría de Ciencia y Técnica-UNS (PGI 24/M093/04) and the Consejo Nacional de Investigaciones Científicas y Técnicas (CONICET-PIP02143/00) is gratefully acknowledged.

## References

- [1] J.T. Reading, J.J. Newport, *Mater. Prot.* 5 (1966) 15.
- [2] W.M. Carroll, C.B. Breslin, *Corros. Sci.* 33 (1992) 1161.
- [3] M.G.A. Khedr, A.M.S. Lashien, *Corros. Sci.* 33 (1992) 137.
- [4] E. Aragon, L. Cazenave-Vergez, E. Lanza, A. Giroud, A. Sebaoun, *Br. Corros. J.* 32 (1997) 263.
- [5] C.B. Breslin, L.P. Friery, W.M. Carroll, *Corros. Sci.* 36 (1994) 85.
- [6] A.G. Muñoz, S.B. Saidman, J.B. Bessone, *Corros. Sci.* 44 (2002) 2171.
- [7] C.B. Breslin, W.M. Carroll, *Corros. Sci.* 33 (1992) 1735.
- [8] A.R. Despić, D.M. Drazic, M.M. Purenović, N. Cirović, *J. Appl. Electrochem.* 6 (1976) 527.
- [9] W.M. Carroll, C.B. Breslin, *Corros. Sci.* 33 (1992) 1161.
- [10] H.A. El Shayeb, F.M. Abd El Wahab, S. Zein El Abedin, *Corros. Sci.* 43 (2001) 643.
- [11] C.D.S. Tuck, J.A. Hunter, G.M. Scamans, *J. Electrochem. Soc.* 134 (1987) 2970.
- [12] J.B. Bessone, D.O. Flamini, S.B. Saidman, *Corros. Sci.* 47 (2005) 95.
- [13] D.O. Flamini, S.B. Saidman, J.B. Bessone, *Corros. Sci.* 48 (2006) 1413.
- [14] P.L.I. Cabot, J.A. Garrido, E. Pérez, J. Virgili, *Corros. Sci.* 26 (1986) 357.
- [15] S. Zein El Abedin, F. Endres, *J. Appl. Electrochem.* 34 (2004) 1071.
- [16] W. Rostaker, J.M. Mc Caughey, H. Marcus, *Embrittlement by Liquid Metals*, Reinhold Publishing Co., New York, 1960, p. 19.
- [17] A. Mance, D. Cerović, A. Mihajlović, *J. Appl. Electrochem.* 15 (1985) 415.
- [18] S.B. Saidman, A.G. Muñoz, J.B. Bessone, *J. Appl. Electrochem.* 29 (1999) 245.
- [19] R.C. Hugo, R.G. Hoagland, *Acta Mater.* 48 (2000) 1949.
- [20] J. Hagström, O.V. Mishin, B. Hutchinson, *Scr. Mater.* 49 (2003) 1035.